


Evidence for deconfined $U(1)$ gauge theory at the transition between toric code and double semion

 Maxime Dupont^{1,2}, Snir Gazit³, and Thomas Scaffidi⁴
¹*Department of Physics, University of California, Berkeley, California 94720, USA*
²*Materials Sciences Division, Lawrence Berkeley National Laboratory, Berkeley, California 94720, USA*
³*Racah Institute of Physics and the Fritz Haber Center for Molecular Dynamics, The Hebrew University, Jerusalem 91904, Israel*
⁴*Department of Physics, University of Toronto, Toronto, Ontario M5S 1A7, Canada*
 (Received 28 August 2020; revised 5 January 2021; accepted 13 April 2021; published 30 April 2021)

Building on quantum Monte Carlo simulations, we study the phase diagram of a one-parameter Hamiltonian interpolating between trivial and topological Ising paramagnets in two dimensions, which are dual to the toric code and the double semion. We discover an intermediate phase with stripe order which spontaneously breaks the protecting Ising symmetry. Remarkably, we find evidence that this intervening phase is gapless due to the incommensurability of the stripe pattern and that it is dual to a $U(1)$ gauge theory exhibiting Cantor deconfinement.

 DOI: [10.1103/PhysRevB.103.L140412](https://doi.org/10.1103/PhysRevB.103.L140412)

Introduction. At first sight, nontrivial bosonic symmetry-protected topological (SPT) phases [1–7] look very similar to their trivial counterparts since they share the same symmetries, behave in the same way in the bulk, and do not possess a local order parameter. Several tools were proposed to unveil the differences between these phases, like comparing their edge properties or looking at their entanglement spectrum or their many-body wave function directly [1–12]. Another way is to gauge the protecting symmetry, since each SPT class is dual to a different Dijkgraaf-Witten gauge theory [1–3, 13–15]. As a result, if one attempts to interpolate from one class to the other, something drastic must happen on the way: either a quantum phase transition or an intermediate phase of matter which breaks spontaneously the protecting symmetry.

Exploring quantum phase transitions featuring SPTs is therefore a good place to look for exotic quantum criticality. In fact, transitions between different SPT phases [16–29], and transitions between SPTs and symmetry-broken states [30–40], have both attracted tremendous attention. Most of the existing work on transitions between SPTs has focused on continuous symmetries with “large” symmetry groups such as $O(N)$, and relations with deconfined quantum criticality have been established in that context [21–23, 25, 26, 29, 41–43]. On the other hand, the study of microscopic models with discrete symmetries has mostly been limited to one dimension (1D) [24, 37].

In this Letter, we investigate the quantum phase diagram of a one-parameter Hamiltonian interpolating between trivial and topological Ising (\mathbb{Z}_2) paramagnets in 2D, which are dual [14] to the toric code (TC) [44] and the double semion (DS) [45–48], respectively. Unlike many other transitions between topological phases, this transition cannot be described in terms of anyon condensation [49], and one has to resort to numerical studies [18, 50–52]. Although the double semion model itself has a sign problem that was proven to be irremediable [53, 54], we have developed a sign-problem-free

quantum Monte Carlo algorithm [55] which takes advantage of its SPT formulation. This allows us to access system sizes an order of magnitude larger than previous work, which relied on exact diagonalization [18]. We find evidence for an intermediate incommensurate stripe phase which is dual to a deconfined $U(1)$ gauge theory and which therefore evades Polyakov’s result on the confinement of compact $U(1)$ gauges theories in $(2+1)D$ [56]. This is one of the first observations of “Cantor deconfinement” in a microscopic system [57–61].

Model. A conventional \mathbb{Z}_2 paramagnet is described by the simple Hamiltonian, $\mathcal{H}_{\text{tr}} = -\sum_j \sigma_j^x$, where $\sigma_j^{x,y,z}$ are Pauli matrices that live on the sites j of the triangular lattice [62]. It has a single gapped ground state $|\psi_{\text{tr}}\rangle$, which is an equal superposition of all σ^z configurations. Since domain walls of Ising spins on the triangular lattice form closed nonintersecting domain walls on the dual honeycomb lattice, we can equally think of $|\psi_{\text{tr}}\rangle$ as an equal superposition of all domain wall configurations, see Fig. 1, which we denote symbolically as $|\psi_{\text{tr}}\rangle = \sum_{\text{dw}} |\text{dw}\rangle$ [63].

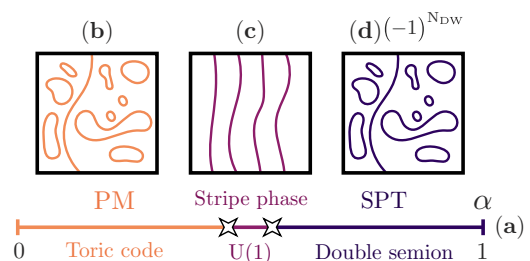


FIG. 1. (a) Phase diagram of the model (1) with intermediate stripe phase centered around $\alpha = 1/2$. Domain walls, which separate up and down regions of σ^z , are represented for typical configurations, in the case of (b) the trivial paramagnetic phase (PM), (c) the stripe ordered phase, and (d) the topological paramagnetic phase (SPT).

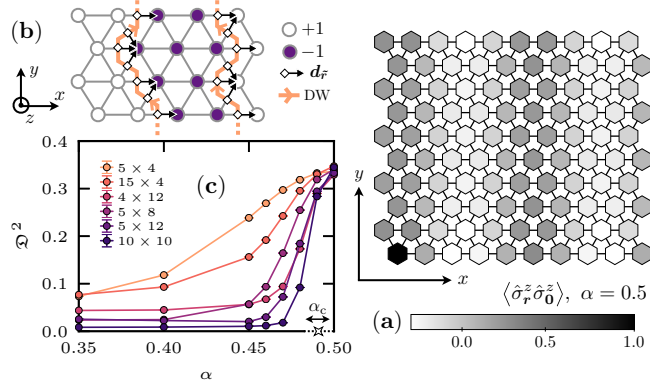


FIG. 2. (a) Stripe structure revealed by $\langle \sigma_r^z \sigma_0^z \rangle$ at $\alpha = 1/2$ for a periodic system of size $N = 10 \times 10$. (b) Sketch of a spin configuration displaying two noncontractible oriented domain walls (orange lines). The black arrows are oriented unit length vectors $\mathbf{d}_{\tilde{r}}$ orthogonal to the domain wall edges \tilde{r} . (c) Square of the order parameter \mathcal{D}^2 defined in Eq. (2) versus α for increasing system sizes. The data is symmetric around $\alpha = 1/2$ for $\alpha > 1/2$.

In 2D, there exists a second type of \mathbb{Z}_2 paramagnet, which is fundamentally different from the trivial one as long as the \mathbb{Z}_2 symmetry is preserved [1–3,14]. A parent Hamiltonian for this topological phase is given by $\mathcal{H}_{\text{top}} = \mathcal{U}^\dagger \mathcal{H}_{\text{triv}} \mathcal{U}$, where $\mathcal{U} = (-1)^{N_{\text{dw}}}$ is a unitary operator giving the parity of the number of domain walls N_{dw} , see the Supplemental Material (SM) for an explicit form of \mathcal{H}_{top} [62]. This Hamiltonian also has a single gapped ground state which is a superposition of all domain wall configurations. The only difference with the trivial paramagnet is that each domain wall comes with a -1 fugacity, i.e., $|\psi_{\text{top}}\rangle = \sum_{\text{dw}} (-1)^{N_{\text{dw}}} |\text{dw}\rangle$. In this work, we interpolate between the two phases with the following one-parameter Hamiltonian,

$$\mathcal{H} = (1 - \alpha)\mathcal{H}_{\text{tr}} + \alpha\mathcal{H}_{\text{top}}, \quad \alpha \in [0, 1]. \quad (1)$$

Intermediate stripe order. We investigate the model (1) by means of quantum Monte Carlo simulations [55,62]. Since $\mathcal{U} = \mathcal{U}^\dagger$, the phase diagram is symmetric around $\alpha = 1/2$, see Fig. 1(a). It is therefore natural to start the analysis at $\alpha = 1/2$, where the real-space two-point correlation $\langle \sigma_r^z \sigma_0^z \rangle$ reveals a stripe structure, as shown in Fig. 2(a) for a prototypical $N = 10 \times 10$ system size.

We observe that the stripe pattern has a period given by $|\mathbf{Q}| \simeq 2\pi/5$, where \mathbf{Q} is the stripe wave vector (we take the lattice spacing equal to unity). However, the orientation of \mathbf{Q} (given by the polar angle φ) and the precise value of the period vary depending on the finite-size system geometry [62]. Depending on the system size, the stripe orientation belongs to one of two sets, which we call “vertical,” with $\varphi = \mathbb{Z}2\pi/6$, and “horizontal,” with $\varphi = (\mathbb{Z} + \frac{1}{2})2\pi/6$. Remarkably, these two sets of orientations are not related by symmetry, which is a good indication that the stripe order is only weakly pinned by the lattice. However, this makes a finite-size analysis based on peaks of the structure factor hazardous.

Instead, we define an order parameter which takes advantage of the domain wall representation. Whereas a paramagnetic phase has domain walls of all shapes and sizes, a perfect stripe phase only has noncontractible domain walls

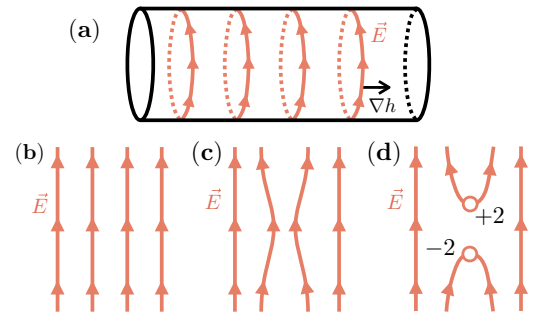


FIG. 3. (a) The domain walls, once oriented, become electric field lines in the gauge description. The orange arrows indicate the direction of the electric field. The surgery process of going from (b) to (d) merges two noncontractible domain walls into one contractible one and only becomes possible away from $\alpha = 1/2$ (due to periodic boundary conditions, the top and bottom of each drawing should be identified). This process creates an electric dipole with charges $q = \pm 2$.

(NCDW) wrapping around the same handle of the torus, see Figs. 1(b)–1(d). Let us define an order parameter \mathcal{D} that is proportional to the number of noncontractible domain walls N_{NCDW} . In order to do this, it is useful to define an integer-valued height field h living on the direct lattice which jumps by one unit every time a domain wall is crossed and whose winding number around a given handle of the torus will give N_{NCDW} . First, we give the same (arbitrary) orientation to each NCDW: For example, for vertical stripes, we choose an “upwards” orientation for each of them, see Figs. 2(b) and 3(a) [62]. This turns each domain wall strand into a vector which we call $\mathbf{E}_{\tilde{r}}$ in anticipation of a gauge interpretation given later (\tilde{r} is an edge of the dual lattice). We can then define the vector field giving the gradient of h : $\nabla h \equiv \mathbf{d}_{\tilde{r}} = \mathbf{E}_{\tilde{r}} \times \mathbf{z}$, where \mathbf{z} is the unit vector perpendicular to the plane.

A macroscopic number of NCDWs translates into a macroscopic tilt for the height field along the direction perpendicular to the domain walls. The squared norm of the tilt, defined as

$$\mathcal{D}^2 = \left\langle \frac{1}{N} \sum_{\tilde{r}} \mathbf{d}_{\tilde{r}} \right\rangle^2, \quad (2)$$

can thus be used as (the square of) our order parameter [64]. For a perfectly ordered stripe phase, there is a simple relation with the stripe wave vector: $\mathcal{D}^2 = (3/2\pi)^2 \mathbf{Q}^2$. As shown in Fig. 2(c) at $\alpha = 1/2$, it takes a finite value $\mathcal{D}^2 \simeq 0.3$ almost independently of the system size. Away from that point, our simulations do not allow us to draw a definite conclusion but from general arguments developed in the following, we expect a finite intermediate ordered phase centered around $\alpha = 1/2$, albeit very small [62]. In fact, the extrapolation of the data as $N \rightarrow +\infty$ is consistent with a jump of \mathcal{D}^2 around $\alpha_c \approx 0.48$ – 0.49 , suggestive of a first order transition between the stripe phase and the paramagnetic phase (and symmetrically at $\alpha_c \approx 0.51$ – 0.52 for the topological side).

Field theory. Following previous works on stripe magnetism [65] and quantum dimer models [58,66–70], we posit that the coarse-grained height field gives the phase of the local magnetization, $m^z(\mathbf{r}) = |m^z| \cos(\pi h(\mathbf{r}))$, and that it is

described by the Lagrangian,

$$\mathcal{L} = \frac{1}{2}(\partial_\tau h)^2 + V[h] + \lambda \cos(2\pi h),$$

$$V[h] = \frac{\rho_2}{2}(\nabla h)^2 + \frac{\rho_4}{2}(\nabla^2 h)^2 + \frac{g_4}{2}(\nabla h)^4 + \mathcal{L}_6, \quad (3)$$

where we have kept implicit the term which accounts for vortices of h . The stripe phase occurs for $\rho_2 < 0$, for which minimizing $V[h]$ leads to a tilt of the height field: $h(\mathbf{r}, \tau) = \pi^{-1} \mathbf{Q} \cdot \mathbf{r} + \delta h(\mathbf{r}, \tau)$, where δh are the fluctuations around the perfectly tilted configuration. The orientation of \mathbf{Q} is determined by the lowest order terms allowed on a triangular lattice: $\mathcal{L}_6 = -g_6 |\nabla h|^6 \cos(6\varphi) - g_{12} |\nabla h|^{12} \cos(12\varphi)$, where φ is the polar angle of ∇h . Since we find both ‘‘vertical’’ and ‘‘horizontal’’ stripes for finite-size systems, we can conclude that g_6 is subdominant compared to g_{12} , leading to two different sets of six minima with almost degenerate values of $V[h]$.

Two different scenarios are possible in order to melt the stripe order. The first one is to tune ρ_2 to zero, which continuously tunes $\mathbf{Q} \rightarrow \mathbf{0}$ until the multicritical Lifshitz (also known as Rokhsar-Kivelson) point $\rho_2 = 0$ [58,66–72]. The second one is to fix ρ_2 but to increase the vortex fugacity, whose proliferation should mark the phase transition to a paramagnetic phase. We propose that this second scenario is the one at play at α_c .

Neglecting λ for now, a long wavelength expansion around one of the minima of $V[h]$ leads to the following Goldstone theory,

$$\mathcal{L} = \frac{1}{2}(\partial_\tau \delta h)^2 + \frac{v_L^2}{2}(\partial_L \delta h)^2 + \frac{v_T^2}{2}(\partial_T \delta h)^2, \quad (4)$$

where L and T stand for the direction longitudinal and transverse to \mathbf{Q} , respectively [73]. The corresponding emergent continuous $U(1)$ symmetry is given by $h \rightarrow h + c$ with $c \in \mathbb{R}$ and describes the longitudinal translation of the stripe pattern with respect to the lattice.

We note that Eq. (3) is dual to a compact $U(1)$ gauge theory for an electric field given by $\mathbf{E} = \mathbf{z} \times \nabla h$ [58,66–69,74,75]. Due to ρ_2 being negative, this theory has an unconventional ‘‘Mexican hat’’ electric energy density which goes like $-\mathbf{E}^2 + \mathbf{E}^4$. This favors a finite density of electric field lines in the ground state, which correspond to the noncontractible domain walls of the stripe phase, see Fig. 3(a).

An expansion around this configuration leads to the photon of Eq. (4). A vertex operator of the type $e^{i2\pi p h}$ maps to a monopole of charge p , and a vortex for h of vorticity q maps to a charge- q electric charge [69]. We also provide in the SM a more microscopic justification for a $U(1)$ gauge theory description of the stripe phase [62].

We now turn our attention to λ , following Ref. [58]. This term imposes discrete values for the height field and corresponds to the addition of $p = 1$ monopoles in the gauge theory. When \mathbf{Q} is incommensurate, λ is irrelevant, and the gapless mode of Eq. (4) survives. This gapless regime is therefore dual to a deconfined $U(1)$ gauge theory, in which test charges experience logarithmic interactions. By contrast, when \mathbf{Q} is commensurate, λ is relevant and gaps out the photon, leading to a confined phase. As we will now show, we find good numerical evidence for a gapless Goldstone boson described by Eq. (4), and we thus surmise that λ is irrelevant,

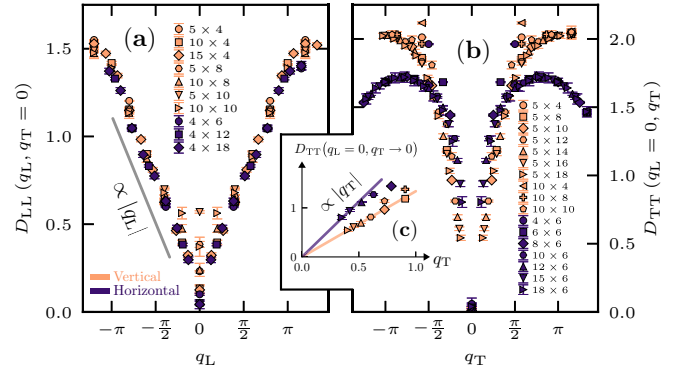


FIG. 4. $D_{ab}(\mathbf{q})$ at $\alpha = 1/2$ for various system sizes ($L_x \times L_y$) leading to vertical (orange) and horizontal (violet) stripes. (a) Longitudinal correlation $D_{LL}(q_L, q_T = 0) \propto |q_L|$ for $q_L \rightarrow 0$ and (b) transverse correlation $D_{TT}(q_L = 0, q_T) \propto |q_T|$ for $q_T \rightarrow 0$, in good agreement with Eq. (6). (c) Same data as (b) for the smallest q_T value for each system size, highlighting agreement with the linear prediction.

or very weakly relevant [76], leading to a deconfined $U(1)$ gauge theory.

We probe the Goldstone boson by computing numerically the following two-point function:

$$D_{ab}(\mathbf{q}) = \sum_{\vec{r}} e^{-i\mathbf{q} \cdot \vec{r}} (\langle d_{\vec{r}}^a d_{\vec{0}}^b \rangle - \langle d_{\vec{r}}^a \rangle \langle d_{\vec{0}}^b \rangle), \quad (5)$$

which is displayed in Fig. 4 at $\alpha = 1/2$, see also SM [62]. Identifying $d_{\vec{r}}$ with the height gradient ∇h , one can derive from Eq. (4) the following prediction [62]:

$$D_{ab}(\mathbf{q}) = \frac{q_a q_b}{2\sqrt{(v_L q_L)^2 + (v_T q_T)^2}}. \quad (6)$$

Note that, in the gauge picture, this is nothing but an electric field correlator [77]. The linear behavior $D_{aa}(q_a, q_b = 0) \sim q_a/2v_a$ for $q_a \rightarrow 0$ is observed in Fig. 4, and we estimate the velocities to be $v_L \simeq 1.2$ and $v_T \simeq 0.3$. Based on this, we extract the following field theory parameters (3): $g_6 \simeq 0$, $g_{12} \simeq 6.5$, $\rho_2 \simeq -0.72$, and $g_4 \simeq 2.25$ [62].

Melting the stripe order. Now that we have a good picture of the stripe order at $\alpha = 1/2$, we can ask how this order gives way to a trivial (respectively topological) paramagnet, when the parameter $\delta\alpha \equiv 1/2 - \alpha$ is tuned to positive (respectively negative) values. Terms proportional to $\delta\alpha$ are the only ones allowing spin flips that change the number of domain walls by ± 1 [62]. Therefore, at $\delta\alpha = 0$, the number of noncontractible domain walls is almost [78] conserved (see numerical evidence in the SM [62]), and the physics is simply described by their vibrations with Eq. (4).

By contrast, for $\delta\alpha \neq 0$, it becomes possible to create contractible domain walls, either from the vacuum or by doing surgery on two noncontractible domain walls, see Figs. 3(b)–3(d). As $|\delta\alpha|$ is increased, these contractible domain walls will proliferate, eventually leading to a condensate of domain walls of all shapes and sizes, i.e., a paramagnetic phase. The negative sign of $\delta\alpha$ on the topological side ensures that each contractible domain wall occurs with the appropriate -1 factor.

As seen in Fig. 3(d) (see also SM [62]), in the gauge picture, a contractible domain wall can be described as a ± 2 electric dipole created to screen the background electric field [79]. This means that $\delta\alpha$ controls the fugacity of ± 2 electric dipoles and the transition to the paramagnetic phases occurs when these charges condense, giving rise to a “Higgs” phase. Since the condensation of charge q particles in a $U(1)$ gauge theory leads to a \mathbb{Z}_q gauge theory [80–83], we recover that the paramagnetic phases are dual to \mathbb{Z}_2 gauge theories, as expected. The condensation of charge-2 matter in a $(2+1)$ D compact $U(1)$ gauge theory was studied before in the case of $\rho_2 > 0$, in which case the $U(1)$ gauge theory is confined due to monopoles [67,80,84–86]. However, to the best of our knowledge, the nature of this transition in the case of $\rho_2 < 0$ has not been considered before and is left for future work.

Note that $q = \pm 2$ are the smallest dynamical charges allowed by the Hamiltonian since $q = \pm 1$ charges would require a dangling domain wall configuration (called π -flux excitation), which are only allowed as static excitations in the TC/DS models. In fact, the $q = \pm 1$ charge survives as one of the gapped quasiparticles of the Higgs phases: It becomes the bosonic e excitation of TC and one of the semions of DS [14].

The other excitation to survive in the Higgs phases is the $p = 1/2$ monopole, which is dual to $\cos(\pi h)$ in the height language and is created by σ_j^z in the original microscopic model. The fact that such a fractional monopole is allowed can be traced back to the nontrivial mapping between Ising spins and domain walls: Translating all domain walls by one inter-domain-wall separation is a good symmetry for the domain walls ($h \rightarrow h + 1$) but not for the spins (since up and down regions are interchanged in the process). The $p = 1/2$ monopole is denoted m and is bosonic in both toric code and double semion [14].

Discussion. Naively, one might have expected an intermediate phase which breaks a discrete symmetry to be gapped and dual to a confined theory. This would have been the case for a ferromagnetic phase for example, for which confinement is a natural consequence of the fact that only short domain walls exist. We have found instead a phase which breaks the Ising symmetry but that has nevertheless long, fluctuating domain walls which allow for a dual deconfined theory.

Finally, our sign-problem-free Monte Carlo algorithm enables us to add a variety of other terms in the Hamiltonian and to study other classes of SPT protected by discrete symmetries [55]. This could enable us to tune ρ_2 towards the quantum Lifshitz point and to study the “Devil’s staircase” of commensurate-incommensurate transitions predicted to happen on the way [58,59]. Another potentially nearby multicritical point could be QED₃ with $N_f = 2$ [87,88], which was predicted to describe the transition between toric code and double semion in the presence of SU(2) symmetry [89]. The closely related deconfined quantum critical point of the J - Q model [90] was in fact recently shown to appear at the tip of a helical valence bond phase which resembles the stripe phase presented in this work [61].

Acknowledgments. We are grateful to F. Alet, N. Bultinck, X. Cao, S. Capponi, E. Fradkin, B. Kang, A. Paramekanti, D. Poilblanc, F. Pollmann, P. Pujol, A. W. Sandvik, R. Vasseur, C. Xu, and L. Zou for interesting discussions. M.D. was supported by the US Department of Energy, Office of Science, Office of Basic Energy Sciences, Materials Sciences and Engineering Division under Contract No. DE-AC02-05-CH11231 through the Scientific Discovery through Advanced Computing (SciDAC) program (KC23DAC Topological and Correlated Matter via Tensor Networks and Quantum Monte Carlo). S.G. acknowledges support from the Israel Science Foundation, Grant No. 1686/18. T.S. acknowledges the financial support of the Natural Sciences and Engineering Research Council of Canada (NSERC), in particular the Discovery Grant No. [RGPIN-2020-05842], the Accelerator Supplement [RGPAS-2020-00060], and the Discovery Launch Supplement [DGECR-2020-00222]. This research used the Lawrence Livermore National Laboratory computational cluster resource provided by the IT Division at the Lawrence Berkeley National Laboratory (Supported by the Director, Office of Science, Office of Basic Energy Sciences, of the US Department of Energy under Contract No. DE-AC02-05CH11231). This research also used resources of the National Energy Research Scientific Computing Center (NERSC), a US Department of Energy Office of Science User Facility operated under Contract No. DE-AC02-05CH11231. T.S. contributed to this work prior to joining Amazon.

-
- [1] X. Chen, Z.-C. Gu, Z.-X. Liu, and X.-G. Wen, Symmetry-protected topological orders in interacting bosonic systems, *Science* **338**, 1604 (2012).
- [2] X. Chen, Z.-C. Gu, Z.-X. Liu, and X.-G. Wen, Symmetry protected topological orders and the group cohomology of their symmetry group, *Phys. Rev. B* **87**, 155114 (2013).
- [3] X. Chen, Z.-X. Liu, and X.-G. Wen, Two-dimensional symmetry-protected topological orders and their protected gapless edge excitations, *Phys. Rev. B* **84**, 235141 (2011).
- [4] Y.-M. Lu and A. Vishwanath, Theory and classification of interacting integer topological phases in two dimensions: A chern-simons approach, *Phys. Rev. B* **86**, 125119 (2012).
- [5] Z. Bi, A. Rasmussen, K. Slagle, and C. Xu, Classification and description of bosonic symmetry protected topological phases with semiclassical nonlinear sigma models, *Phys. Rev. B* **91**, 134404 (2015).
- [6] F. Pollmann, A. M. Turner, E. Berg, and M. Oshikawa, Entanglement spectrum of a topological phase in one dimension, *Phys. Rev. B* **81**, 064439 (2010).
- [7] F. Pollmann, E. Berg, A. M. Turner, and M. Oshikawa, Symmetry protection of topological phases in one-dimensional quantum spin systems, *Phys. Rev. B* **85**, 075125 (2012).
- [8] Y.-Z. You, Z. Bi, A. Rasmussen, K. Slagle, and C. Xu, Wave Function and Strange Correlator of Short-Range Entangled States, *Phys. Rev. Lett.* **112**, 247202 (2014).
- [9] Z. Ringel and S. H. Simon, Hidden order and flux attachment in symmetry-protected topological phases: A Laughlin-like approach, *Phys. Rev. B* **91**, 195117 (2015).
- [10] T. Scaffidi and Z. Ringel, Wave functions of symmetry-protected topological phases from conformal field theories, *Phys. Rev. B* **93**, 115105 (2016).

- [11] J. C. Wang, L. H. Santos, and X.-G. Wen, Bosonic anomalies, induced fractional quantum numbers, and degenerate zero modes: The anomalous edge physics of symmetry-protected topological states, *Phys. Rev. B* **91**, 195134 (2015).
- [12] L. H. Santos and J. Wang, Symmetry-protected many-body aharonov-bohm effect, *Phys. Rev. B* **89**, 195122 (2014).
- [13] R. Dijkgraaf and E. Witten, Topological gauge theories and group cohomology, *Commun. Math. Phys.* **129**, 393 (1990).
- [14] M. Levin and Z.-C. Gu, Braiding statistics approach to symmetry-protected topological phases, *Phys. Rev. B* **86**, 115109 (2012).
- [15] J. C. Wang, Z.-C. Gu, and X.-G. Wen, Field-Theory Representation of Gauge-Gravity Symmetry-Protected Topological Invariants, Group Cohomology, and Beyond, *Phys. Rev. Lett.* **114**, 031601 (2015).
- [16] T. Grover and A. Vishwanath, Quantum phase transition between integer quantum hall states of bosons, *Phys. Rev. B* **87**, 045129 (2013).
- [17] Y.-M. Lu and D.-H. Lee, Quantum phase transitions between bosonic symmetry-protected topological phases in two dimensions: Emergent qed_3 and anyon superfluid, *Phys. Rev. B* **89**, 195143 (2014).
- [18] S. C. Morampudi, C. von Keyserlingk, and F. Pollmann, Numerical study of a transition between z_2 topologically ordered phases, *Phys. Rev. B* **90**, 035117 (2014).
- [19] L. Tsui, F. Wang, and D.-H. Lee, Topological versus landau-like phase transitions, [arXiv:1511.07460](https://arxiv.org/abs/1511.07460).
- [20] L. Tsui, H.-C. Jiang, Y.-M. Lu, and D.-H. Lee, Quantum phase transitions between a class of symmetry protected topological states, *Nucl. Phys. B* **896**, 330 (2015).
- [21] Y.-Z. You, Z. Bi, D. Mao, and C. Xu, Quantum phase transitions between bosonic symmetry-protected topological states without sign problem: Nonlinear sigma model with a topological term, *Phys. Rev. B* **93**, 125101 (2016).
- [22] Y.-Y. He, H.-Q. Wu, Y.-Z. You, C. Xu, Z. Y. Meng, and Z.-Y. Lu, Bona fide interaction-driven topological phase transition in correlated symmetry-protected topological states, *Phys. Rev. B* **93**, 115150 (2016).
- [23] Y.-Z. You, Y.-C. He, A. Vishwanath, and C. Xu, From bosonic topological transition to symmetric fermion mass generation, *Phys. Rev. B* **97**, 125112 (2018).
- [24] L. Tsui, Y.-T. Huang, H.-C. Jiang, and D.-H. Lee, The phase transitions between $zn \times zn$ bosonic topological phases in $1+1d$, and a constraint on the central charge for the critical points between bosonic symmetry protected topological phases, *Nucl. Phys. B* **919**, 470 (2017).
- [25] S. Geraedts and O. I. Motrunich, Lattice realization of a bosonic integer quantum hall state–trivial insulator transition and relation to the self-dual line in the easy-plane nccp1 model, *Phys. Rev. B* **96**, 115137 (2017).
- [26] Z. Bi and T. Senthil, Adventure in Topological Phase Transitions in $3 + 1$ -d: Non-Abelian Deconfined Quantum Criticalities and a Possible Duality, *Phys. Rev. X* **9**, 021034 (2019).
- [27] N. Bultinck, Uv perspective on mixed anomalies at critical points between bosonic symmetry-protected phases, *Phys. Rev. B* **100**, 165132 (2019).
- [28] S. Gozel, D. Poilblanc, I. Affleck, and Frédéric Mila, Novel families of $su(n)$ aklt states with arbitrary self-conjugate edge states, *Nucl. Phys. B* **945**, 114663 (2019).
- [29] T.-S. Zeng, D. N. Sheng, and W. Zhu, Continuous phase transition between bosonic integer quantum hall liquid and a trivial insulator: Evidence for deconfined quantum criticality, *Phys. Rev. B* **101**, 035138 (2020).
- [30] J. P. Kestner, B. Wang, J. D. Sau, and S. Das Sarma, Prediction of a gapless topological haldane liquid phase in a one-dimensional cold polar molecular lattice, *Phys. Rev. B* **83**, 174409 (2011).
- [31] T. Grover and A. Vishwanath, Quantum criticality in topological insulators and superconductors: Emergence of strongly coupled majoranas and supersymmetry, [arXiv:1206.1332](https://arxiv.org/abs/1206.1332).
- [32] A. Keselman and E. Berg, Gapless symmetry-protected topological phase of fermions in one dimension, *Phys. Rev. B* **91**, 235309 (2015).
- [33] L. Zhang and F. Wang, Unconventional Surface Critical Behavior Induced by a Quantum Phase Transition from the Two-Dimensional Affleck-Kennedy-Lieb-Tasaki Phase to a Néel-Ordered Phase, *Phys. Rev. Lett.* **118**, 087201 (2017).
- [34] T. Scaffidi, D. E. Parker, and R. Vasseur, Gapless Symmetry-Protected Topological Order, *Phys. Rev. X* **7**, 041048 (2017).
- [35] D. E. Parker, T. Scaffidi, and R. Vasseur, Topological luttinger liquids from decorated domain walls, *Phys. Rev. B* **97**, 165114 (2018).
- [36] D. E. Parker, R. Vasseur, and T. Scaffidi, Topologically Protected Long Edge Coherence Times in Symmetry-Broken Phases, *Phys. Rev. Lett.* **122**, 240605 (2019).
- [37] R. Verresen, R. Moessner, and F. Pollmann, One-dimensional symmetry protected topological phases and their transitions, *Phys. Rev. B* **96**, 165124 (2017).
- [38] R. Verresen, N. G. Jones, and F. Pollmann, Topology and Edge Modes in Quantum Critical Chains, *Phys. Rev. Lett.* **120**, 057001 (2018).
- [39] R. Verresen, R. Thorngren, N. G. Jones, and F. Pollmann, Gapless topological phases and symmetry-enriched quantum criticality, [arXiv:1905.06969](https://arxiv.org/abs/1905.06969).
- [40] C. M. Duque, H.-Y. Hu, Y.-Z. You, V. Khemani, R. Verresen, and R. Vasseur, Topological and symmetry-enriched random quantum critical points, *Phys. Rev. B* **103**, L100207 (2021).
- [41] T. Senthil, A. Vishwanath, L. Balents, S. Sachdev, and Matthew P. A. Fisher, Deconfined quantum critical points, *Science* **303**, 1490 (2004).
- [42] C. Wang, A. Nahum, M. A. Metlitski, C. Xu, and T. Senthil, Deconfined Quantum Critical Points: Symmetries and Dualities, *Phys. Rev. X* **7**, 031051 (2017).
- [43] Y. Q. Qin, Y.-Y. He, Y.-Z. You, Z.-Y. Lu, A. Sen, A. W. Sandvik, C. Xu, and Z. Y. Meng, Duality between the Deconfined Quantum-Critical Point and the Bosonic Topological Transition, *Phys. Rev. X* **7**, 031052 (2017).
- [44] A.Yu. Kitaev, Fault-tolerant quantum computation by anyons, *Ann. Phys. (NY)* **303**, 2 (2003).
- [45] M. A. Levin and X.-G. Wen, String-net condensation: A physical mechanism for topological phases, *Phys. Rev. B* **71**, 045110 (2005).
- [46] M. Iqbal, D. Poilblanc, and N. Schuch, Semionic resonating valence-bond states, *Phys. Rev. B* **90**, 115129 (2014).
- [47] O. Buerschaper, S. C. Morampudi, and F. Pollmann, Double semion phase in an exactly solvable quantum dimer model on the kagome lattice, *Phys. Rev. B* **90**, 195148 (2014).

- [48] Y. Qi, Z.-C. Gu, and H. Yao, Double-semion topological order from exactly solvable quantum dimer models, *Phys. Rev. B* **92**, 155105 (2015).
- [49] F.J. Burnell, Anyon condensation and its applications, *Annu. Rev. Condens. Matter Phys.* **9**, 307 (2018).
- [50] C.-Y. Huang and T.-C. Wei, Detecting and identifying two-dimensional symmetry-protected topological, symmetry-breaking, and intrinsic topological phases with modular matrices via tensor-network methods, *Phys. Rev. B* **93**, 155163 (2016).
- [51] M. Iqbal, K. Duivenvoorden, and N. Schuch, Study of anyon condensation and topological phase transitions from a \mathbb{Z}_4 topological phase using the projected entangled pair states approach, *Phys. Rev. B* **97**, 195124 (2018).
- [52] W.-T. Xu and G.-M. Zhang, Tensor network state approach to quantum topological phase transitions and their criticalities of \mathbb{Z}_2 topologically ordered states, *Phys. Rev. B* **98**, 165115 (2018).
- [53] M. B. Hastings, How quantum are non-negative wavefunctions? *J. Math. Phys.* **57**, 015210 (2016).
- [54] A. Smith, O. Golan, and Z. Ringel, Intrinsic sign problems in topological quantum field theories, *Phys. Rev. Research* **2**, 033515 (2020).
- [55] M. Dupont, S. Gazit, and T. Scaffidi, From trivial to topological paramagnets: The case of \mathbb{Z}_2 and \mathbb{Z}_2^2 symmetries in two dimensions, *Phys. Rev. B* **103**, 144437 (2021).
- [56] A.M. Polyakov, Quark confinement and topology of gauge theories, *Nucl. Phys. B* **120**, 429 (1977).
- [57] L. S. Levitov, Equivalence of the Dimer Resonating-Valence-Bond Problem to the Quantum Roughening Problem, *Phys. Rev. Lett.* **64**, 92 (1990).
- [58] E. Fradkin, D. A. Huse, R. Moessner, V. Oganesyan, and S. L. Sondhi, Bipartite rokhsar-kivelson points and cantor deconfinement, *Phys. Rev. B* **69**, 224415 (2004).
- [59] S. Papanikolaou, K. S. Raman, and E. Fradkin, Devil's staircases, quantum dimer models, and stripe formation in strong coupling models of quantum frustration, *Phys. Rev. B* **75**, 094406 (2007).
- [60] T. Schlittler, T. Barthel, Grégoire Misguich, J. Vidal, and Rémy Mosseri, Phase Diagram of an Extended Quantum Dimer Model on the Hexagonal Lattice, *Phys. Rev. Lett.* **115**, 217202 (2015).
- [61] B. Zhao, J. Takahashi, and A. W. Sandvik, Multicritical Deconfined Quantum Criticality and Lifshitz Point of a Helical Valence-Bond Phase, *Phys. Rev. Lett.* **125**, 257204 (2020).
- [62] See Supplemental Material at <http://link.aps.org/supplemental/10.1103/PhysRevB.103.L140412> for the explicit form for the topological Hamiltonian, information regarding the quantum Monte Carlo simulations, an intuitive justification for the apparition of a stripe order, details about the prescription used to orient contractible domain walls, additional numerical data as well as additional details regarding the field theory. See also Refs. [1–3,14,53–55,58,66–70,74,75,91–96] therein.
- [63] Strictly speaking, since the mapping from spins to domain walls is 2 to 1, there should be an extra sum over the two possible spin orientations for a given domain wall configuration.
- [64] A similar order parameter, called winding number, was used for a stripe phase on the triangular lattice in Ref. [97].
- [65] G. Grinstein, Anisotropic sine-gordon model and infinite-order phase transitions in three dimensions, *Phys. Rev. B* **23**, 4615 (1981).
- [66] A. Vishwanath, L. Balents, and T. Senthil, Quantum criticality and deconfinement in phase transitions between valence bond solids, *Phys. Rev. B* **69**, 224416 (2004).
- [67] E. Ardonne, P. Fendley, and E. Fradkin, Topological order and conformal quantum critical points, *Ann. Phys. (NY)* **310**, 493 (2004).
- [68] R. Moessner, S. L. Sondhi, and E. Fradkin, Short-ranged resonating valence bond physics, quantum dimer models, and ising gauge theories, *Phys. Rev. B* **65**, 024504 (2001).
- [69] E. Fradkin, *Field Theories of Condensed Matter Physics*, Field Theories of Condensed Matter Physics (Cambridge University Press, Cambridge, UK, 2013).
- [70] R. Moessner and Kumar S Raman, Quantum dimer models, in *Introduction to Frustrated Magnetism* (Springer, Berlin, Heidelberg, 2011), pp. 437–479.
- [71] D. S. Rokhsar and S. A. Kivelson, Superconductivity and the Quantum Hard-Core Dimer Gas, *Phys. Rev. Lett.* **61**, 2376 (1988).
- [72] S. V. Isakov, P. Fendley, A. W. W. Ludwig, S. Trebst, and M. Troyer, Dynamics at and near conformal quantum critical points, *Phys. Rev. B* **83**, 125114 (2011).
- [73] Note that the transverse stiffness term $(\partial_\tau \delta h)^2$ only arises due to \mathcal{L}_6 , and the transverse velocity is therefore parametrically different from the longitudinal one [98].
- [74] R. Youngblood, J. D. Axe, and B. M. McCoy, Correlations in ice-rule ferroelectrics, *Phys. Rev. B* **21**, 5212 (1980).
- [75] E. Fradkin and S. Kivelson, Short range resonating valence bond theories and superconductivity, *Mod. Phys. Lett. B* **04**, 225 (1990).
- [76] A possible scenario would be a commensurate order with a very small gap, since it was shown that the gap is exponentially small in the weak-tilt regime [58].
- [77] D. A. Huse, W. Krauth, R. Moessner, and S. L. Sondhi, Coulomb and Liquid Dimer Models in Three Dimensions, *Phys. Rev. Lett.* **91**, 167004 (2003).
- [78] The only process which can change the number of domain walls is a rare event in which three domain walls come close and combine into one.
- [79] This process of pair creation can be seen as a condensed matter version of the Schwinger effect [99].
- [80] E. Fradkin and S. H. Shenker, Phase diagrams of lattice gauge theories with higgs fields, *Phys. Rev. D* **19**, 3682 (1979).
- [81] S. Sachdev and N. Read, Large n expansion for frustrated and doped quantum antiferromagnets, *Int. J. Mod. Phys. B* **05**, 219 (1991).
- [82] C. Mudry and E. Fradkin, Separation of spin and charge quantum numbers in strongly correlated systems, *Phys. Rev. B* **49**, 5200 (1994).
- [83] M. de Wild Propitius, Topological interactions in broken gauge theories, Ph.D. thesis, University of Amsterdam, 1995.
- [84] O. I. Motrunich and T. Senthil, Exotic Order in Simple Models of Bosonic Systems, *Phys. Rev. Lett.* **89**, 277004 (2002).
- [85] T. Senthil and O. Motrunich, Microscopic models for fractionalized phases in strongly correlated systems, *Phys. Rev. B* **66**, 205104 (2002).
- [86] J. Smiseth, E. Smørgrav, F. S. Nogueira, J. Hove, and A. Sudbø, Phase structure of (2+1)-dimensional compact lattice gauge theories and the transition from mott insulator to fractionalized insulator, *Phys. Rev. B* **67**, 205104 (2003).

- [87] X. Y. Xu, Y. Qi, L. Zhang, F. F. Assaad, C. Xu, and Z. Y. Meng, Monte Carlo Study of Lattice Compact Quantum Electrodynamics with Fermionic Matter: The Parent State of Quantum Phases, *Phys. Rev. X* **9**, 021022 (2019).
- [88] N. Karthik and R. Narayanan, Numerical determination of monopole scaling dimension in parity-invariant three-dimensional noncompact qed, *Phys. Rev. D* **100**, 054514 (2019).
- [89] M. Barkeshli, Transitions between chiral spin liquids and Z2 spin liquids, [arXiv:1307.8194](https://arxiv.org/abs/1307.8194).
- [90] A. W. Sandvik, Evidence for Deconfined Quantum Criticality in a Two-Dimensional Heisenberg Model with Four-Spin Interactions, *Phys. Rev. Lett.* **98**, 227202 (2007).
- [91] F. Becca and S. Sorella, *Quantum Monte Carlo Approaches for Correlated Systems* (Cambridge University Press, Cambridge, UK, 2017).
- [92] A. W. Sandvik, Computational studies of quantum spin systems, *AIP Conf. Proc.* **1297**, 135 (2010).
- [93] A. W. Sandvik, *Many-Body Methods for Real Materials, Modeling and Simulation*, edited by E. Pavarini, E. Koch, and S. Zhang, Verlag des Forschungszentrum Jülich, Vol. 9 (Modeling and Simulation, Jülich, Germany, 2019).
- [94] Z. Dai and A. Nahum, Quantum criticality of loops with topologically constrained dynamics, *Phys. Rev. Research* **2**, 033051 (2020).
- [95] W. Selke, The anni model — theoretical analysis and experimental application, *Phys. Rep.* **170**, 213 (1988).
- [96] M. Kardar and Y.-C. Zhang, Scaling of Directed Polymers in Random Media, *Phys. Rev. Lett.* **58**, 2087 (1987).
- [97] A. Smerald, S. Korshunov, and Frédéric Mila, Topological Aspects of Symmetry Breaking in Triangular-Lattice Ising Antiferromagnets, *Phys. Rev. Lett.* **116**, 197201 (2016).
- [98] L. Radzihovsky and A. Vishwanath, Quantum Liquid Crystals in an Imbalanced Fermi Gas: Fluctuations and Fractional Vortices in Larkin-Ovchinnikov States, *Phys. Rev. Lett.* **103**, 010404 (2009).
- [99] J. Schwinger, On gauge invariance and vacuum polarization, *Phys. Rev.* **82**, 664 (1951).